DOI: 10.1478/AAPP.98S1A1

AAPP | Atti della Accademia Peloritana dei Pericolanti
Classe di Scienze Fisiche, Matematiche e Naturali
ISSN 1825-1242

Vol. 98, No. S1, A1 (2020)

EFFECTS OF TOPOLOGICAL DISORDER ON THERMODYNAMIC AND VIBRATIONAL PROPERTIES OF AMORPHOUS SOLIDS

GIOVANNA D'ANGELO [a b] * AND GIUSEPPE CARINI [a b]

ABSTRACT. The disordered topology introduces additional degrees of freedom in the structure of amorphous solids mainly enhancing the local atomic mobility. This gives rise to substantial and amazing changes of the physical properties of these systems compared to the corresponding crystals, *i.e.*, solids having the same stoichiometry, but over an ordered structure. In this article, the possible connection between the thermodynamic and vibrational aspects of glasses and the topological disorder is considered, emphasizing the most significant differences between crystalline and amorphous solids having the same stoichiometry.

1. Introduction

The most striking characteristic, which differentiates amorphous solids from crystalline ones, is the absence of the first order phase transition associated with crystallization from the melt. It is replaced by a continuous transition of the extensive thermodynamic variables, such as volume V, entropy S and enthalpy H, measured as a function of temperature T with a gradual change of slope over of a temperature region defined "the glass transition region". A further important peculiarity of amorphous solids, mostly for its remarkable universality, is the excess of low-energy vibrational excitations, which exist beside phonons and take their origin from the disordered topology. The nature of the above mechanisms is quite far from a clear and exhaustive understanding. As clearly emphasized by Anderson (1995), "The deepest and most interesting unsolved problem in solid state theory is probably the theory of the nature of the glass and the glass transition". To illustrate the paramount effects of topological disorder on thermodynamic properties of amorphous solids, we present here some new results concerning the comparison between the specific heat capacities of vitreous (v-B_2O_3) and crystalline (c-B_2O_3) boron trioxide over the very large temperature interval between 0.4 and 900 K. Raman spectra are also reported to discuss the molecular structure of the glasses.

The structure of v-B_2O_3, one of the main prototypes of strong glasses, is quite different from that of its crystalline polymorph α-B_2O_3 (c-B_2O_3). The crystal is formed from planar ribbons of BO_3 triangles (Gurr *et al.* 1970), while the glass evidences also the formation

of boroxol rings (B_3O_6) (Joo *et al.* 2000; Umari and Pasquarello 2005; Zwanziger 2005; Ferlat *et al.* 2008), these super-structural units being composed by three corner sharing BO_3 planar triangles which are the basic units building up the network. Boroxol rings are formed during the melt-quenching process and about 3 over 4 boron atoms belong to rings (Umari and Pasquarello 2005) in the glass quenched at atmospheric pressure. They swell substantially the network and contribute to lower the density of v-B_2O_3, 1826 kg/m^3 against 2560 kg/m^3 of crystalline c-B_2O_3, (Gurr *et al.* 1970) with a decrease of 40%, very much higher than those usually experienced by most glasses. It is worth noting that crystallization of boron trioxide from a dry melt at atmospheric pressure has never been observed. Despite its resistance to crystallization at atmospheric pressure, crystals of α-B_2O_3 may readily be obtained at pressures higher than 1 GPa (Mackenzie and Claussen 1961).

2. Experimental details

Crystalline samples were obtained by fusing $^{11}B_2O_3$ glasses at 1280 °C under a pressure of 4 GPa for about 15 min and then pressure-quenched to room temperature. X-ray diffraction pattern of polycrystalline samples gave well-defined peaks, typical of trigonal α-B_2O_3 (Gurr *et al.* 1970). The temperature behaviour of the heat capacity of c-B_2O_3 over the temperature range between room temperature and 900 K (quite above the melting temperature $T_m = 723$ K) is reported in Fig. 1(a). The specific heat capacities of the samples were determined using a Mettler differential scanning calorimeter (DSC). Discs of each sample of mass approximately 25 mg were encapsulated in aluminium pans and subjected to the same thermal cycles with a heating rate of 10 K/min by maintaining the experimental chamber under a controlled atmosphere of nitrogen. Calibrations of the DSC output were performed using a standard sapphire sample. For the low temperature specific-heat measurements, the standard thermal relaxation method in a ^{4}He cryostat between 1.5 and 30 K and in a ^{3}He cryostat between 0.4 and 2 K was applied. Raman scattering measurements were performed at room temperature using the 5145 Å line of an argon-ion laser with a power of 300 mW and a Yobin Yvon U-1000 double monocromator. Polarized vertical–vertical (VV) spectra were measured in a 90 ° scattering geometry with an incident beam polarized vertically with respect to the scattering plane. The resolution of the experimental set-up was 1 cm^{-1}.

3. Thermal properties

The heat capacity of the crystal increases monotonically with increasing temperature up to about 723 K, showing for further increase of T a huge endothermic peak associated to the melting of the solid. Quite differently, the glass having the same stoichiometry, but a disordered structure (X-ray diffraction revealed no sign of crystallization), shows a heat capacity which above 300 K varies smoothly with increasing temperature, except for the usual endothermic peak at T_g which overlaps with a sudden jump from glassy to liquid-like behaviour through the glass transition temperature, Fig. 1(b). The complete absence of melting endotherms in the explored temperature interval indicates that the glass can be regarded as a homogeneous amorphous system. The glass transition temperature of v-B_2O_3 was established as the inflection point of the endothermal jump and indicated by an arrow in Fig. 1(b). After the first heating run of both c-B_2O_3 and v-B_2O_3, they were quenched to

room temperature inside the calorimeter and subsequently reheated to above the liquidus temperature. The second thermal run of the crystal does not reveal any sign of endothermic peak, showing a behaviour of the heat capacity very close to that of the glass (1(a)).

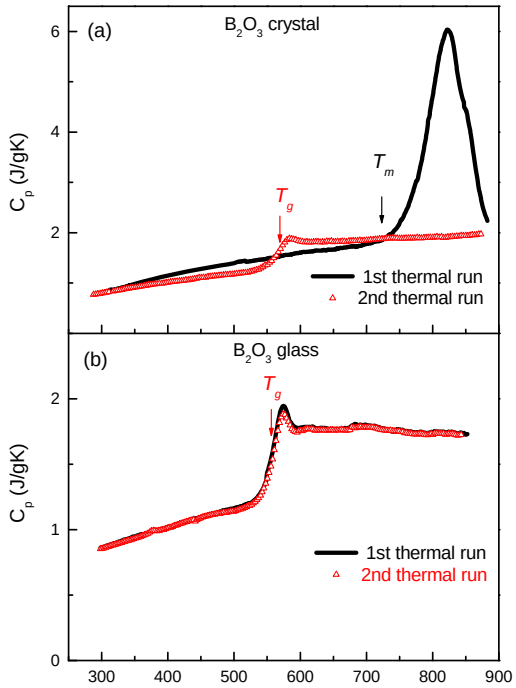

FIGURE 1. *a)* Temperature variation of the heat capacity in crystalline B_2O_3 obtained by DSC at a scan rate of 20 K min^{-1}: first thermal run, solid line; second thermal run, open triangles. Arrows show the melting temperature $T_m = 723$ K and the glass transition temperature $T_g = 570$ K. *b)* Temperature variation of the heat capacity in glassy B_2O_3 obtained by DSC at a scan rate of 20 K min^{-1}: first thermal run, solid line; second thermal run, open triangles. The arrow shows the glass transition temperature $T_g = 560$ K.

This fact reveals the glass-forming ability of the system, that can be understood as a measure of its metastability and confirms the above-mentioned resistance to crystallization of boron trioxide at atmospheric pressure. The second thermal run on the glass revealed a behaviour of the heat capacity very close to that observed in the prior thermal run, Fig. 1(b), evidencing only a slightly smaller endothermic peak and a higher T_g . Due to the metastable state of a glass, it is expected that a property such as T_g should be dependent on prior

thermal history. Although this was found to be true in this investigation, the fluctuations in the measurements attributable to thermal history were really very small.

4. Excess of low-energy vibrational dynamics: the boson peak

As discussed above, amorphous solids exhibit an excess of low-energy vibrational modes over the classical Debye density of states whose nature is quite far from a clear and exhaustive understanding. These collective modes range between 0.1 and 3 THz and contribute to (i) the boson peak (BP) in inelastic light (Raman) and neutron scattering spectra, (ii) the excess low temperature (1-20 K) specific heat capacity C_p having the shape of a broad hump when reported as C_p/T^3 and (iii) the plateau of the thermal conductivity $k(T)$ at around 10 K (Nakayama 2002; D'Angelo *et al.* 2009, 2010; Crupi *et al.* 2012).

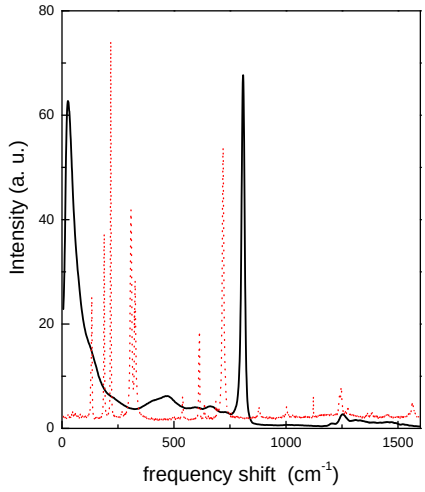

FIGURE 2. Raman spectra of v-B_2O_3 (solid line) and c-B_2O_3 (dotted line) for VV polarization. Above 970 cm^{-1} the *y* scale has been expanded by a factor of 4.

All these experimental findings exhibit a remarkable universality and are usually ascribed to an excess of low-energy excitations, which exist beside phonons and take their origin from the disordered topology of amorphous structures. The existence of correlations between these excitations and the peculiar peak observed in the static structure factor of all investigated glasses (the "First sharp diffraction peak", FSDP) has been also extensively investigated. It seems that while the BP arises from intermediate-range ordering within the

network units of the system, the FSDP arises from the ordering of voids between such units (Crupi *et al.* 2015).

4.1. Low-frequency Raman scattering. Raman spectra of v-B_2O_3 and c-B_2O_3 between 6 and 1600 cm^{-1} are reported in Fig. 2 for VV (polarized) configuration. The comparison shows that the two main features observed in the glass, *i.e.*, the BP at 26 $cm^{-1}$and the band at 808 cm^{-1}, are fully missing in the crystal. The BP has been ascribed to low frequency librations of coupled boroxol rings (Carini Jr *et al.* 2013, 2015), while the line at 808 cm^{-1} arises from a localized breathing-type vibration of oxygen atoms inside the plane of boroxol rings (Carini Jr *et al.* 2018). The lines observed in c-B_2O_3 prove that its structure is built on infinite chains of BO_3 triangles (Gurr *et al.* 1970) and does not contain boroxol rings. The first feature observed in the crystal is the optical mode at 132 cm^{-1}, also visible as a shoulder on the high frequency tail of the BP in the glass. These observations indicate a strong correlation between the boroxol ring population and the vibrations underlying the BP, disclosing that this excess modes must be associated to low-energy vibrations of these glassy structural units.

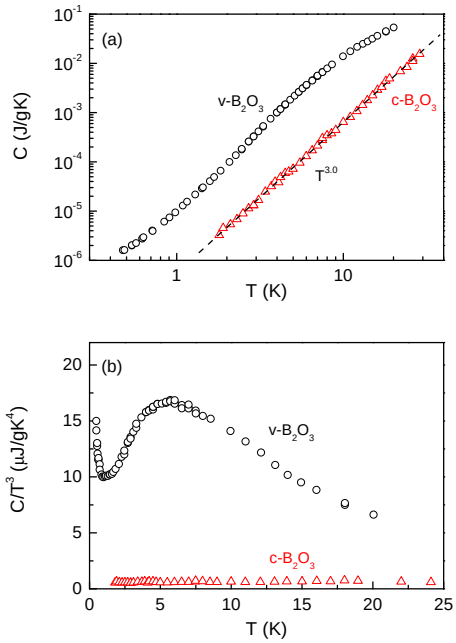

FIGURE 3. *a)* The temperature dependence of the specific heat capacity C_p in v-B_2O_3 (open circle symbol) and crystalline B_2O_3 (open triangle symbol). The dotted line represents a fit to the data between 2 K and 8 K of c-B_2O_3, which gives a $T^{3.0}$-behavior. *b)* The temperature dependence of $C_p(T)/T^3$ for v-B_2O_3 and c-B_2O_3; the symbols are the same as in (a).

4.2. Low-temperature specific heat. The low temperature specific heat capacity $C(T)$ of v-B_2O_3 is compared with that of c-B_2O_3 in Fig. 3(a). In crystalline dielectric solid, phonons dominate the thermal properties: $C(T)$ of c-B_2O_3 strictly follows the Debye T^3 -law (dotted line in Fig. 3(a)) giving a Debye temperature Θ_D=621 K. Glassy B_2O_3 shows an excess $C(T)$ over the heat capacity of the crystalline sample. When plotted as $C(T)/T^3$ vs T, Fig. 3(b), it results the characteristic shape of a broad peak (also defined as the calorimetric BP) at about 5.7 K with a magnitude substantially larger than the elastic Debye contributions $C_D(T)$. These evidences lead us to assign the large excess $C_p(T)$ observed in v-B_2O_3 and the vibrational dynamics underlying the BP to low-energy modes mainly arising from boroxol rings. These superstructural glassy units are missing in the crystal, whose low-energy vibrational dynamics is fully described by the Debye model (Figs. 3(a) and 3(b)). The rings are formed due to the poor atomic packing of the glassy network and can be connected either via a single oxygen atom bridging two rings or via one or several planar BO_3 triangles. Out-of-plane rigid librations of planar boroxol rings are believed to be the source for the excess of low-energy vibrations determining both the Raman and calorimetric BP. It is worth noting that observation of low-energy librations of coupled glassy units is not limited to v-B_2O_3, but it has been also found in other prototype glasses, such as v-SiO_2 (Buchenau *et al.* 1986; Hehlen *et al.* 2000) and v-Se (Bermejo *et al.* 1994).

5. Conclusions

The results discussed above show some important effects of topological disorder on the thermodynamic properties of amorphous solids, emphasizing substantial differences between crystalline and amorphous solids having the same stoichiometry. A more or less general understanding of "disordered amorphous state" has now been established, paving the way to technology with the synthesis of new materials useful for a very wide range of applications, but the disappearance of a thermodynamic phenomenon, like the phase transition of the first order marking the fusion of a crystal, is still far from being fully understood.

References

Anderson, P. W. (1995). "Through the Glass Lightly". *Science* **267**(5204), 1615–1616. DOI: 10.1126/science.267.5204.1615-e.

Bermejo, F. J., Enciso, E., Criado, A., Martinez, J. L., and Garcia-Hernández, M. (1994). "Thermal transport in glassy selenium: The role of low-frequency librations". *Physical Review B* **49**(13), 8689. DOI: 10.1103/PhysRevB.49.8689.

Buchenau, U., Prager, M., Nücker, N., Dianoux, A. J., Ahmad, N., and Phillips, W. A. (1986). "Low-frequency modes in vitreous silica". *Physical Review B* **34**(8), 5665. DOI: 10.1103/PhysRevB.34.5665.

Carini Jr, G., Carini, G., D'Angelo, G., Federico, M., and Romano, V. (2018). "Boroxol ring modification driven by plastic deformations of compacted B_2O_3 glasses". *Journal of Non-Crystalline Solids* **492**, 102–107. DOI: 10.1016/j.jnoncrysol.2018.03.047.

Carini Jr, G., Carini, G., D'Angelo, G., Gilioli, E., and Vasi, C. (2015). "Origin of excess low-energy vibrations in densified B_2O_3 glasses". *Philosophical Magazine* **95**(24), 2596–2606. DOI: 10.1080/14786435.2015.1067733.

Carini Jr, G., Carini, G., D'Angelo, G., Tripodo, G., Di Marco, G., Vasi, C., and Gilioli, E. (2013). "Influence of packing on low energy vibrations of densified glasses". *Physical Review Letters* **111**(24), 245502. DOI: 10.1103/PhysRevLett.111.245502.

Crupi, C., Carini, G., González, M., and D'Angelo, G. (2015). "Origin of the first sharp diffraction peak in glasses". *Physical Review B* **92**(13), 134206. DOI: 10.1103/PhysRevB.92.134206.

Crupi, C., D'Angelo, G., and Vasi, C. (2012). "Low-energy vibrational dynamics of cesium borate glasses". *The Journal of Physical Chemistry B* **116**(22), 6499–6505. DOI: 10.1021/jp301230s.

D'Angelo, G., Carini, G., Crupi, C., Koza, M., Tripodo, G., and Vasi, C. (2009). "Boson peak in alkaline borate glasses: Raman spectroscopy, neutron scattering, and specific-heat measurements". *Physical Review B* **79**(1), 014206. DOI: 10.1103/PhysRevB.79.014206.

D'Angelo, G., Crupi, C., Tripodo, G., and Salvato, G. (2010). "Relation between low-temperature thermal conductivity and the specific heat of cesium borate glasses". *The Journal of Physical Chemistry B* **114**(7), 2467–2475. DOI: 10.1021/jp907152y.

Ferlat, G., Charpentier, T., Seitsonen, A. P., Takada, A., Lazzeri, M., Cormier, L., Calas, G., and Mauri, F. (2008). "Boroxol rings in liquid and vitreous B_2O_3 from first principles". *Physical Review Letters* **101**(6), 065504. DOI: 10.1103/PhysRevLett.101.065504.

Gurr, G. E., Montgomery, P. W., Knutson, C. D., and Gorres, B. T. (1970). "The crystal structure of trigonal diboron trioxide". *Acta Crystallographica Section B: Structural Crystallography and Crystal Chemistry* **26**(7), 906–915. DOI: 10.1107/S0567740870003369.

Hehlen, B., Courtens, E., Vacher, R., Yamanaka, A., Kataoka, M., and Inoue, K. (2000). "Hyper-Raman scattering observation of the boson peak in vitreous silica". *Physical Review Letters* **84**(23), 5355. DOI: 10.1103/PhysRevLett.84.5355.

Joo, C., Werner-Zwanziger, U., and Zwanziger, J. W. (2000). "The ring structure of boron trioxide glass". *Journal of Non-Crystalline Solids* **261**(1-3), 282–286. DOI: 10.1016/S0022-3093(99)00609-2.

Mackenzie, J. D. and Claussen, W. F. (1961). "Crystallization and phase relations of boron trioxide at high pressures". *Journal of the American Ceramic Society* **44**(2), 79–81. DOI: 10.1111/j.1151-2916.1961.tb15354.x.

Nakayama, T. (2002). "Boson peak and terahertz frequency dynamics of vitreous silica". *Reports on Progress in Physics* **65**(8), 1195. DOI: 10.1088/0034-4885/65/8/203.

Umari, P. and Pasquarello, A. (2005). "Fraction of boroxol rings in vitreous boron oxide from a first-principles analysis of Raman and NMR spectra". *Physical Review Letters* **95**(13), 137401. DOI: 10.1103/PhysRevLett.95.137401.

Zwanziger, J. W. (2005). "The NMR response of boroxol rings: a density functional theory study". *Solid State Nuclear Magnetic Resonance* **27**(1-2), 5–9. DOI: 10.1016/j.ssnmr.2004.08.004.

[a] Università degli Studi di Messina
Dipartimento di Scienze Matematiche e Informatiche, Scienze Fisiche e Scienze della Terra
Contrada Papardo, 98166 Messina, Italy

[b] Consiglio Nazionale delle Ricerche
Istituto Processi Chimico-Fisici, Sezione di Messina
Viale F. Stagno d'Alcontres 37, I-98158, Messina, Italy

* To whom correspondence should be addressed | email: gdangelo@unime.it

Paper contributed to the international workshop entitled "Glasses and polymers: the science of disorder",
which was held in Messina, Italy (15–16 November 2018), under the patronage of the *Accademia Peloritana dei Pericolanti*
Manuscript received 8 November 2019; published online 1 October 2020